International Journal of Nanomedicine

Dovepress
open access to scientific and medical research

Open Access Full Text Article

ORIGINAL RESEARCH

# *Daphnia magna* and *Xenopus laevis* as in vivo models to probe toxicity and uptake of quantum dots functionalized with gH625

This article was published in the following Dove Press journal:
International Journal of Nanomedicine
4 April 2017
Number of times this article has been viewed

Emilia Galdiero[1]
Annarita Falanga[2]
Antonietta Siciliano[1]
Valeria Maselli[1]
Marco Guida[1]
Rosa Carotenuto[1]
Margherita Tussellino[1]
Lucia Lombardi[3]
Giovanna Benvenuto[4]
Stefania Galdiero[2]

[1]Department of Biology, [2]Department of Pharmacy and CiRPEB, University of Naples Federico II, [3]Department of Experimental Medicine, Second University of Naples, [4]Stazione Zoologica Anton Dohrn, Villa Comunale, Napoli, Italy

**Abstract:** The use of quantum dots (QDs) for nanomedicine is hampered by their potential toxicologic effects and difficulties with delivery into the cell interior. We accomplished an in vivo study exploiting *Daphnia magna* and *Xenopus laevis* to evaluate both toxicity and uptake of QDs coated with the membranotropic peptide gH625 derived from the glycoprotein H of herpes simplex virus and widely used for drug delivery studies. We evaluated and compared the effects of QDs and gH625-QDs on the survival, uptake, induction of several responsive pathways and genotoxicity in *D. magna*, and we found that QDs coating plays a key role. Moreover, studies on *X. laevis* embryos allowed to better understand their cell/tissue localization and delivery efficacy. *X. laevis* embryos raised in Frog Embryo Teratogenesis Assay-*Xenopus* containing QDs or gH625-QDs showed that both nanoparticles localized in the gills, lung and intestine, but they showed different distributions, indicating that the uptake of gH625-QDs was enhanced; the functionalized QDs had a significantly lower toxic effect on embryos' survival and phenotypes. We observed that *D. magna* and *X. laevis* are useful in vivo models for toxicity and drug delivery studies.

**Keywords:** membranotropic peptide, delivery, blood–brain barrier, nanoparticles, genotoxicity

## Introduction

Nanotechnology is rapidly developing and new materials are being produced for a variety of applications. In particular, nanotechnology applied to medicine is expected to bring significant advances in diagnosis and treatment of diseases. The primary goal of research in this field is obtainment of platforms for specific drug delivery and targeting, and reduction of toxicity while preserving the therapeutic effects, safety and biocompatibility.[1]

Metal nanoparticles (MNPs) have been extensively used in medical and biologic research with applications in targeted drug delivery, optical bioimaging and so on.[2–5] With widespread applications, it has become fundamental to investigate their safety and, in fact, the mechanisms triggering their cytotoxicity remain mostly unclear. Toxicity is strictly dependent on internalization pathways, with intracellular aggregation and accumulation into endolysosomal compartments being the leading cause of nanotoxicity, due to nanoparticle (NP) degradation and release of metal ions. Some other possible consequences of exposure to MNPs are production of reactive oxygen species (ROS), genotoxicity and apoptosis, as well as mitochondrial damage and metallic ion production.[6] Size, shape and coating together with dose, route of administration and exposure are key factors that determine the degree of toxicity.

Correspondence: Stefania Galdiero
Department of Pharmacy and CiRPEB, University of Naples Federico II, Via Mezzocannone 16, 80134 Napoli, Italy
Tel +39 08 1253 4503
Fax +39 08 1253 4560
Email stefania.galdiero@unina.it

submit your manuscript | www.dovepress.com
Dovepress
http://dx.doi.org/10.2147/IJN.S127226

The internalization pathways of MNPs involve canonic endocytic pathways, which means they end in lysosomes where degradative processes take place and might be responsible of cytotoxicity. MNPs internalization pathways may determine their localization inside the cell and their toxic potential, which means that their toxicity is correlated not only to the physicochemical features but also to the microenvironmental conditions they come into contact during internalization.

A possible strategy to change their mechanism of internalization is the use of membranotropic cell-penetrating peptides, which present the ability to cross biologic membranes without cell rupture, but only partially involving endocytic pathways.[7,8] The coupling of cell-penetrating peptides to MNPs provides a good strategy for a substantial improvement of cellular uptake, enabling them to deliver a large variety of cargo molecules for therapy and diagnosis.

The peptide gH625, identified in our laboratory,[9] belongs to the glycoprotein H of herpes simplex virus type I and is a membranotropic domain which contributes to the fusing of the viral and the cellular membranes.[10,11] This peptide has proved to exhibit exceptional vector properties[9] and has been shown to be essentially internalized by a nonendocytic pathway avoiding endosomal entrapment.[7,12–17] In recent studies, it was also shown to be able to cross the blood–brain barrier in vitro and in vivo.[18] gH625 is, therefore, a very good delivery vector[9] and its coupling to NPs may be exploited to change their internalization mechanism and in case of MNPs, to avoid or reduce their toxicity.

Quantum dots (QDs) represent a kind of MNPs. Their use as fluorescent probes for bioimaging has led to several applications such as single-membrane receptor tracking, multicolor immunofluorescence, in vivo cell tracking or cell lineage imaging.[19] Nevertheless, their use as specific probes is restricted to extracellular targets in living cells or to immunofluorescence imaging of fixed cells. This drawback derives mainly from the hurdles of cell uptake and maintaining the QDs freely diffusing and unaggregated once inside the living cells. To settle these drawbacks, various internalization strategies and QD surface chemistries have been tried with limited success. We recently reported about the functionalization of CdSe QDs with gH625, which enhanced their uptake essentially involving nonendocytic pathways.[20]

The novelty and complexity of this subject together with the lack of homogeneity in the kind of NPs and methods to analyze the complex interactions with living systems make it difficult to provide standardized information on toxicity. Literature is overloaded of examples of in vitro experiments showing MNPs toxicity for several cell types.[21–23] In vivo experiments have been reported to further support the toxicity of MNPs (dysfunctions of the intestinal apparatus in embryonic zebra fish models, defects in the embryonic development of *Xenopus laevis*, phenotypic modifications in the progeny of *Drosophila melanogaster* and a decrease in body weight, red blood cells, hematocrit and DNA damage in mice).[24–28]

The in vivo studies and the potential effects on public health and ecosystems are key to understanding the real applicability of a delivery strategy. Animal welfare, ethical issues and economics have rendered fundamental use of in vivo assays on invertebrates.[29] These organisms present less-developed cortical and sensorial systems and fast tissue regeneration. Moreover, invertebrates of the aquatic environment are undoubtedly at risk of exposure to any pollutant; thus, they are widely used in bioassays for ecotoxicity and we propose that although their organs are different from those of mammals, arthropods and other crustaceans, studies on this organism may provide initial information not only on ecotoxicity but also on the pharmacologic applicability of nanoplatforms for drug delivery to modify according to the specific disease to treat.

*Daphnia magna* bioassays are recommended over other models for assessment of aquatic toxicity because of increased oral exposure from filter feeding.[30,31] Here, we propose that bioassays with *D. magna* are viable and advantageous also in pharmacologic studies. For example, *D. magna* has been widely used to investigate drugs with cardiac activity (such as acetylcholine, tetraethyl pyrophosphate, pilocarpine, adrenaline and rotenone).[32] Another advantage of using *D. magna* in research is that its transparency[33] allows to obtain insights into animal physiology; in fact, researchers may apply optical methods to not only visualize the physiologic functions but also measure several different parameters simultaneously[34] with a noninvasive method.[35] Moreover, simplicity to culture them, short life cycle, discrete growth, easy handling and low cost of maintenance make *D. magna* bioassays highly advantageous. These important features may help in understanding the mechanisms of action of nanodelivery platforms for humans.

Embryos of zebrafish (*Danio rerio*) have been successfully used as whole-organism in vivo bioassay systems to study human pathologies and to discover novel therapeutics.[36] Because of the physiologic differences and the considerable evolutionary distance between zebrafish and humans, it is not easy to directly translate from zebrafish to mammalian systems; some of these problems may be avoided by turning to animal models that are evolutionary closer to humans. *X. laevis* is an adaptable tool that has been previously exploited

to complement the more extensively used rodent model in cancer research. The high degree of conservation of fundamental mechanisms among vertebrates, the possibility to perform experiments in *X. laevis* in shorter times and with smaller expenses than those with mouse models and the reduction of problems correlated with animal welfare and ethical issues make *X. laevis* a key tool to provide initial observations that can be extended to mammalian models including humans.[37,38] Amphibian embryos have already been used as an alternative vertebrate animal model for the discovery of potential therapeutic agents.[39] *Xenopus* embryonic development is rapid and occurs outside the mother's body in simple salt solutions; moreover, the developing larvae and tadpoles become transparent, facilitating the detection of tissue and organ defects by visual inspection under a dissection microscope. A close similarity to mammals is present at the level of organ organization and structure, such as heart, kidneys, lymphatics and immune system.[40] *X. laevis* has been widely exploited to determine the effects of pollutants in aquatic larvae, contributing to the unraveling of their eventual toxicity and harmfulness. Moreover, *X. laevis* embryos are also an excellent model system to assess new tools for delivering and detecting NPs because of their size, rapid development and possibility of mapping cell fates. Thus, it has emerged as a powerful model organism not only for developmental biology but also for understanding the delivery of molecules and as predictor of health effects.

This report aimed to investigate the potential of functionalized QDs to be taken up by *D. magna* and by *X. laevis* (during embryogenesis) without inducing cytotoxicity. Moreover, *D. magna* and *X. laevis* embryos may be used as in vivo models to study toxicity and drug delivery and may prove to be useful for drug discovery screenings.

# Methods

## Peptide synthesis

The peptide gH625-GGG was synthesized using standard solid-phase 9-fluorenylmethoxycarbonyl method as previously reported.[10] Briefly, peptides were obtained using a Wang (0.58 mmol $g^{-1}$) resin by consecutive deprotection (30% piperidine) and coupling (2 equivalents of amino acid, 2 equivalents of 1-Hydroxybenzotriazole (HOBT)/3-[Bis(dimethylamino)methyliumyl]-3H-benzotriazol-1-oxide hexafluorophosphate (HBTU) and 4 equivalents of DIPEA) steps. Peptides were fully deprotected and cleaved from the resin with trifluoroacetic acid (TFA)/5% thioanisole/3% ethandithiol/2% anisole as scavengers for 90 min. The crude peptides were precipitated with ethyl ether, filtered and lyophilized. Analysis was performed by liquid chromatography–mass spectrometry using a gradient of acetonitrile (0.1% TFA) in water (0.1% TFA) from 20% to 80% in 10 min; purifications were performed by semi-preparative reversed-phase high-performance liquid chromatography. The purified peptide was obtained with good yields (~60%).

## Synthesis and characterization of functionalized QDs

Solution of peptides in 1-ethyl-3(3-dimethylamino-propyl)-carbodiimide, hydrochloride and *N*-hydroxysuccinimide (molar ratio of 4:4:1) was prepared in phosphate-buffered saline (PBS) buffer at pH 7.4. QDs 525NC (amine), composed of CdSe, were purchased from eBioscience and conjugated with the preactivated peptides in a molar ratio of 1:200 in 2-(N-Morpholino)ethanesulfonic acid (MES) buffer at pH 5.5 for 3 h. The absorbance spectra of peptide-QDs and unconjugated QDs were measured using NanoDrop 2000C Spectrophotometer (Thermo Fisher Scientific) in the same conditions. The final solution obtained was 117 nM QDs and 500 µM gH625. For all reported experiments, we compared the results using the concentration of the QDs; thus, the peptide concentration can be calculated from the mother solution concentration.

Dynamic light scattering was performed using a Malvern Nanosizer Nano ZS (Malvern Instruments, Worcestershire, UK), with an He–Ne laser 4 mW source operating at 633 nm and the scattering angle fixed at 173° on colloidal dispersions. The measurements were conducted at 25°C in triplicate.

## *D. magna* culture

*D. magna* was cultured in the Ecotoxicology Research Laboratory of the Department of Biology of University of Naples Federico II for several generations following recommended procedures of Organisation for Economic Co-operation and Development (OECD) Guidelines 211. Briefly, *D. magna* were maintained in culture medium M4[41] under a light:dark photoperiod of 16:8 h at 20°C±2°C and fed daily with algae (*Raphidocelis subcapitata*). The medium was renewed twice a week. Neonates (<24 h old) were isolated for exposures and used in all experiments of this study.

## *D. magna* acute toxicity test

Acute toxicity experiments were performed to determine the acute lethal toxicity of QDs and gH625-QDs on *D. magna*. Four replicates of five daphnids were exposed to 0.3, 0.6, 1.2, 2.5, 5 and 10 nM of QDs and gH625-QDs. All details of the acute toxicity test using daphnids were in accordance with OECD Guidelines 211. Immobilization was quantified at

48 h and animals that were unable to swim within 15 s after gentle shaking were considered dead. International Organization for Standardization (ISO) artificial freshwater,[42] containing $CaCl_2 \cdot 2H_2O$ (294 mg·L$^{-1}$), $MgSO_4 \cdot 7H_2O$ (123 mg·L$^{-1}$), $NaHCO_3$ (64.8 mg·L$^{-1}$) and KCl (5.75 mg·L$^{-1}$), was used for the preparation of test solutions and for the control medium.[43] Temperature, conductivity, dissolved oxygen and pH were measured in the test media before and after 48 h of exposure.

## Uptake experiment on *D. magna*

Based on the concentration incurring 50% effect of test species ($EC_{50}$) values determined, a concentration of 5 nM was chosen so that the majority of daphnids were viable and the NPs showed some effect on stress and survival. Twenty adult *D. magna* were transferred to each well containing different concentrations of QDs and gH625-QDs and the control (Ctl), until 24 h. Each treatment was sampled at five time points (30′, 60′, 90′, 6 h and 24 h). Images of live *D. magna* were obtained using fluorescence microscope (Leica DMLB microscope with digital camera Leica DFC340FX; Leica Microsystems, Nussloch, Germany), analyzed and compared. The spectrum of QDs was distinct from that of *D. magna* and no interference was observed.[44,45]

## ROS and antioxidant enzyme analysis

The amount of ROS produced in *D. magna* was measured with $H_2$DCFDA.[46] The final concentration of $H_2$DCFDA was 10 mM. Live *D. magna* were used for the determination of ROS. After 24 h of exposure to QDs and gH625-QDs at each concentration, 10 daphnids were transferred to 1 mL of $H_2$DCFDA for 4 h at 20°C in the dark. ROS quantity was monitored by fluorescence (excitation wavelength of 350 nm and emission wavelength of 600 nm).

Twenty exposed and nonexposed daphnids were homogenized in sucrose buffer (0.25 M sucrose, 0.1 M Tris–HCl, pH 8.6) and centrifuged (4°C, 20,800 × *g* for 10 min). Enzymatic activities of superoxide dismutase (SOD) and catalase (CAT) were measured in the supernatant.

CAT activities were calculated and expressed as decrease in absorbance at 240 nm due to $H_2O_2$ consumption using a commercial kit (Sigma-Aldrich Co., St Louis, MO, USA) and according to the manufacturer's protocol.

SOD activity was measured by the inhibition of cytochrome *c* reduction using a SOD assay kit-WST (Sigma-Aldrich Co.) according to the manufacturer's instructions. The increased absorbance corresponding to the reduction of cytochrome *c* by $O_2^-$ was measured at 550 nm in three to five separate replicates.

## Protein quantification

Protein concentration was quantified spectrophotometrically at 595 nm according to the Bradford method with bovine serum albumin (BSA) as the standard.[47]

## Comet assay

To evaluate whether QDs and gH625-QDs exerted genotoxicity on *D. magna* DNA damage and, in particular, DNA strand breaks, a comet assay was performed. The alkaline comet assay was performed on *D. magna* treated for 48 h with QDs and gH625-QDs (0.3, 0.6, 1.2, 2.5, 5, 10 nM). As described in detail previously,[48] we suspended treated organisms in the homogenization solution (PBS, 20 mM ethylendiaminetetracetic acid [EDTA], 10% dimethyl sulfoxide [DMSO]) where they are mechanically crumbled and filtered (Sigma-Aldrich Co., 100 mm mesh). Slides were treated with a first layer of Normal Melting Point Agarose (1%), a second layer of a Low Melting Point Agarose (1%) mixed with the solution containing the organisms and a third layer of Low Melting Point Agarose, 1%. After solidification, the slides were placed overnight at 4°C in a lysis solution (2.5 M NaCl, 100 mM EDTA, 10 mM Tris, 1% Triton X-100, pH 7.5).

The slides were incubated in an alkaline buffer (300 mM NaOH, 1 mM $Na_2$EDTA [EDTA disodium salt], pH >13) for 30 min. Thereafter, the slides were subjected to electrophoresis for 30 min (25 mV, 300 mA). Finally, the slides were washed twice for 5 min in a neutralization buffer (Tris–HCl 0.4 M, pH 7.5) and stained for 3 h with 4′,6-diamidino-2-phenylindole (DAPI) (50 mg/mL). A fluorescence microscope was used to examine the slides, analyzing a minimum of 50 randomly selected nuclei from each slide and avoiding overlapping figures.

## Daphnia's heart rate

The experiment was performed following an established protocol.[49] Cotton fibers were placed into a concave microscope slide to allow only some movements and to prevent swimming. Any water remaining on the slide was entirely absorbed. A single daphnia was transferred to a slide containing QDs and gH625-QDs at concentrations used in all experiments. After 2 min of acclimatization to the environment, the heart rate was recorded directly by a camera mounted on a stereomicroscope Leica EZ4 HD and connected to a computer.

## *X. laevis* fertilization

Adult *X. laevis* were obtained from Nasco (Fort Atkinson, WI, USA). The guidelines and policies imposed by the

University Animal Welfare Office in agreement with the international rules and in strict accordance with the recommendations in the Guide for the Care and Use of Laboratory Animals of the National Institutes of Health of the Italian Ministry of Health were strictly followed for keeping and using *X. laevis*. Furthermore, the protocol was approved by the Committee on the Ethics of Animal Experiments (Centro Servizi Veterinari) of the University of Naples Federico II (Permit Number: 2016/0003675–01/15/2016). All procedures were performed according to Italian ministerial authorization (DL 116/92 art.7; prot. 2013/0032839) and European regulations on the protection of animals used for experimental and other scientific purposes. For all surgical procedures, ethyl 3-aminobenzoate methanesulfonate (MS222) was used. All trials were adopted to minimize suffering. To obtain eggs and fertilization, *X. laevis* females were injected in the dorsal lymphatic sac with 500 units of gonase (AMSA) in amphibian Ringer solution (111 mM NaCl, 1.3 mM $CaCl_2$, 2 mM KCl and 0.8 mM $MgSO_4$ in 25 mM Hepes, pH 7.8). Fertilized eggs and embryos were obtained by standard insemination methods and staged according to Nieuwkoop and Faber.[50]

## *X. laevis* embryos treatment

The embryos were reared starting from stage 4/8 in Frog Embryo Teratogenesis Assay-*Xenopus* pH 7.4 (106 mM NaCl, 11 mM $NaHCO_3$, 4 mM KCl, 1 mM $CaCl_2$, 4 mM $CaSO_4$, 3 mM $MgSO_4$) solution containing QDs (10 nM) or gH625-QDs (10 nM). All embryos were harvested until stage 45/46. Sibling embryos were used as control.

The embryos' survival and phenotype were checked daily. The embryos did not show any clear sign of distress as sickness, pain or suffering, and neither did they show any other signs as gradual loss of motility or depigmentation of the skin that are the typical signs of suffering for *Xenopus* embryos before dying. During breeding and exposure of *X. laevis* embryos to QDs, we checked the pH of the medium to verify the level of urea and accordingly changed the medium. The embryos were kept at a constant temperature of ~21°C. The mortality percentage was calculated on the number of dead embryos versus their total initial number. The relationship between the control and the treated groups, along with the percentage of dead embryos, was investigated with chi-square test, using the Yate's correction for continuity or the Fisher's exact test.

The phenotypes of embryos were scored when the embryos reached stage 45/46, corresponding to the known stages of anlagen morphogenesis. At stage 40/41, *X. laevis* embryos opened their mouth and ingestion became the main route of NPs intake. Since in the following days the grazing behavior of the larvae became very active, the number of ingested particles increased. Samples for phenotype analysis were photographed using a Leica MZ16F ultraviolet (UV) stereomicroscope, equipped with a Leica DFC 300Fx camera and IM50 Image Manager Software.

To verify the presence of QDs and gH625-QDs, the embryos were fixed in 4% paraformaldehyde (PFA), washed in PBS 1× and embedded in 0.5% gelatin (Sigma-Aldrich Co., G1890). Gelatin blocks were sectioned with a VT1200 S vibrating blade microtome (Leica Microsystems). Fifty micrometer slices were mounted in PBS/glycerol 50% v/v and observed with a Zeiss LSM 510META confocal microscope (excitation HeNe 543 laser and emission filter BP 550–615). Projections shown in this study were produced by recording the confocal image stacks and projecting them in the *z*-axis using ImageJ (1.49v Java 1.6.0_20, National Institutes of Health, USA).

## Determination of length, heart rate and dorsal pigmentation in *X. laevis*

For length determination, the embryos were observed in dorsal position under an MZ16F UV stereomicroscope equipped with eyepiece micrometer. Heart rate was measured by observing the embryos under an MZ16F UV stereomicroscope integrated with light-emitting diode ring light. The number of heartbeats was taken for 30 s, three times each. For pigmentation, the embryos were photographed in dorsal position. From digital image, the areas of pigment covering the brain dorsal portion were cut out and analyzed with Image Pro Plus software version 6.0.0.260 for Windows 2000/XP Professional (Media Cybernetics, Rockville, MD, USA). All the measurements were normalized to the controls for each experiment.

## Data analysis

Tail moment (TM) was used to obtain a quantitative assessment of DNA damage (Comet Score 1.5 Image Analysis; TriTek Corporation, Sumerduck, VA, USA). The median of TM of 50 nuclei per slide was calculated for each sample (treated and control), and the distribution of TM median values was analyzed by Shapiro and Wilk and Kolmogorov and Smirnov tests.[51,52] Levene's test was applied to evaluate variance homogeneity of each sample.

Results are given as mean ± standard error, and effective concentrations to reach 10%, 20% and 50% of the maximum response were calculated by using a nonlinear regression analysis with 95% confidence interval (CI).

The relationship between the control and the treated groups, along with the percentage of dead embryos, was investigated with chi-square test, using the Yate's correction for continuity or the Fisher's exact test. The survival distributions in the control and experimental groups were also assessed in terms of significance using nonparametric Mantel–Cox test.

To evaluate differences among groups, we used analysis of variance parametric test and Kruskal–Wallis nonparametric test[53] with Tukey or Dunn's test for post hoc analysis, respectively. These tests were used to compare all pairs of columns.[54] To obtain the *P*-value, the parametric *t*-test Mann–Whitney was used, always comparing treated embryos to the controls.

# Results

## Characterization of QDs functionalized with gH625

To quantify and confirm peptide conjugation to QDs, UV/vis characterization was done following the tryptophan residues present in the peptide (Figure 1). The analyses allowed us to confirm the conjugation of the peptide on the QDs and to determine the concentration of the mother solution. In particular, the mother solutions for gH625-QDs were 117 nM in QDs and 500 μM in peptide, and for QDs alone it was 117 nM. Dynamic light scattering was performed to determine the size of the QDs and gH625-QDs. Table 1 lists the dimensions at the concentrations used in the experiments.

## Acute toxicity test on *D. magna*

The immobilization of daphnids after 48 h of exposure to QDs and gH625-QDs was compared (Figure 2). As shown in Figure 2 and Table 2, the $EC_{50}$ was not calculated for gH625-QDs (the immobility did not reach 50% even at the highest concentration used); for QDs, the calculated $EC_{50}$ was 1.5 nM.

At the end of exposure time, daphnids exposed to QDs reached 67% of immobilization while those exposed to gH625-QDs reached 15% of immobilization at the highest dose used (10 nM). These data indicate a decreased toxicity of QDs functionalized with gH625. The 48 h $EC_{50}$ value was 1.5 nM (CI: 0.01–0.16) and the $EC_{10}$ value was 0.02 nM for QDs (the range of CI was very wide because the percentage of immobilization already reached 30% at 0.1 nM), while the $EC_{50}$ value for gH625-QDs was not determinable and the $EC_{10}$ value was 1 nM (CI: 0.6–1.0). These data clearly show a nontoxic response to the test organisms for gH625-QDs.

**Table 1** Size measured by DLS, expressed as z-average and PDI

| NPs | Average size (nm) | PDI |
|---|---|---|
| QDs | 120.90±2.37 | 0.35±0.11 |
| gH625-QDs | 171.40±1.27 | 0.35±0.05 |

**Note:** Data are expressed as mean ± SD of three separate experiments for each of the two batch formulations, with at least 13 measurements for each.
**Abbreviations:** NPs, nanoparticles; PDI, polydispersity index; QDs, quantum dots; SD, standard deviation; DLS, dynamic light scattering.

## Genotoxicity on *D. magna*

To evaluate the genotoxicity on *D. magna*, DNA damage and DNA strand breaks were determined using a comet assay. The data showed that treated samples were characterized by

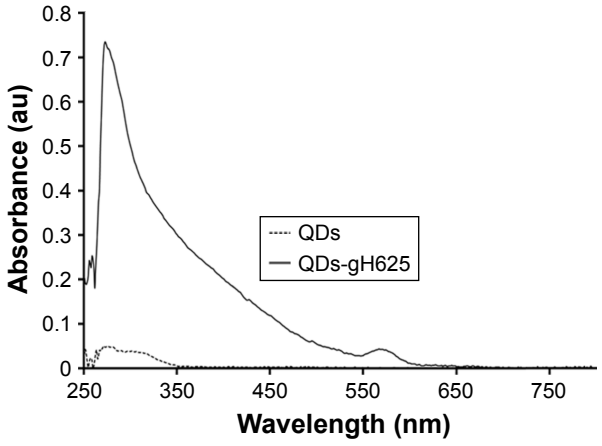


**Figure 1** UV/Vis spectra of gH625-QDs and QDs alone.
**Abbreviations:** QDs, quantum dots; UV/Vis, ultraviolet/visible.

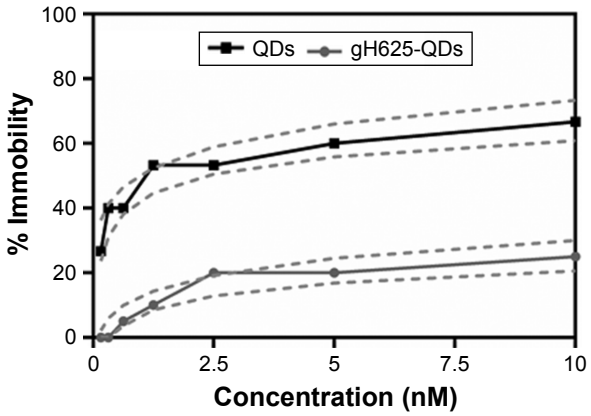


**Figure 2** Immobility of *Daphnia magna* exposed to QDs and gH625-QDs for 48 h; dashed line represents confidence intervals.
**Notes:** The concentrations reported are relative to QDs (the concentration of 10 nM QDs corresponds to a peptide concentration of 43 μM). Data are reported as mean ± SEM (n=9). Bonferroni *post hoc* test following two-way ANOVA versus the QDs group. All the data present significant differences ($P<0.001$).
**Abbreviations:** ANOVA, analysis of variance; QDs, quantum dots; SEM, standard error of the mean.

**Table 2** Mean effective concentration from toxicity tests (95% CI shown in brackets) against exposure to QDs and gH625-QDs for 48 h

| Sample | $EC_{50}$ (95% CI) nM | $EC_{20}$ (95% CI) nM | $EC_{10}$ (95% CI) nM |
|---|---|---|---|
| QDs | 1.5 (0.01–0.16) | ND | ND |
| gH625-QDs | ND | 4.4 (2.5–4.5) | 1.0 (0.6–1.01) |

**Abbreviations:** CI, confidence interval; $EC_{50}$, concentration incurring 50% effect of test species; QDs, quantum dots; ND, not determined.

higher genotoxicity, compared to untreated control samples (Figure 3). TMs increased in *D. magna* exposed to higher doses of QDs in the presence or absence of gH625.

As shown in Figure 3, in cells isolated from *D. magna* and exposed to QDs (concentration between 0.3 and 10 nM), the TM increased gradually with concentration, indicating the occurrence of a dose-dependent DNA damage (y=2.5×–4.5, $R^2$=0.65 for QDs). We observed a similar trend with QDs coated with gH625, with a lower slope (y=1.8×–4.7, $R^2$=0.73 for gH625-QDs). At each concentration, QDs alone were found to be more toxic than when coated with gH625. Median values for the control samples were significantly lower than after treatment, both for QDs and gH625-QDs ($P<0.001$ Kruskal–Wallis analysis of variance rank model). The analysis of median comet metrics from experiments at different exposure rate levels is a valid method to demonstrate QDs genotoxic effect, because there is a clear dose-dependent response with increasing values of TM. Nonparametric test was used to evaluate the difference in time-reliable cell responses for different QD concentrations. We found a statistically significant difference between the TM of each population and the control ($P<0.001$, Kruskal–Wallis test,[55] made one by one population versus control), and between the TM of each population exposed to gH625-QDs or QDs alone. QDs can induce a significant DNA damage, which is reduced when the QDs are in combination with gH625.

## Cardiotoxicity on *D. magna*

*Daphnia* heart rate has been used as a biomarker of physiologic stress, and its increase may be due to low oxygen levels,[56] high temperature[57] or chemical exposure.[58] Both QDs and gH625-QDs altered heartbeat at the highest concentration used; nonetheless, there was not a significant change in heart rate compared to the control (Figure 4). The induction of an increased heart rate in *D. magna* for both QDs and gH625-QDs is also associated with the induction of ROS and a low level of antioxidant enzymes. In fact, it is known that heart rate was affected at much lower concentrations than the results of traditional toxicity tests, including environmental concentration.[59]

## Uptake on *D. magna*

We performed experiments to monitor the uptake and excretion of QDs functionalized and not functionalized with gH625 in order to understand their localization in the daphnid organs. Daphnids naturally ingest particulates from the water column or sediment and have been previously shown to readily uptake and accumulate NPs in the gut within 6–12 h after exposure.[60] We monitored the uptake of QDs and gH625-QDs until 24 h (30′, 60′, 90′, 6 and 24 h; Figure 5). We noticed that *D. magna* actively takes up and excretes QDs; in particular, both the ingestion and the excretion of QDs and gH625-QDs were very fast, probably because of their active filter-feeding mechanisms (Figure 5).

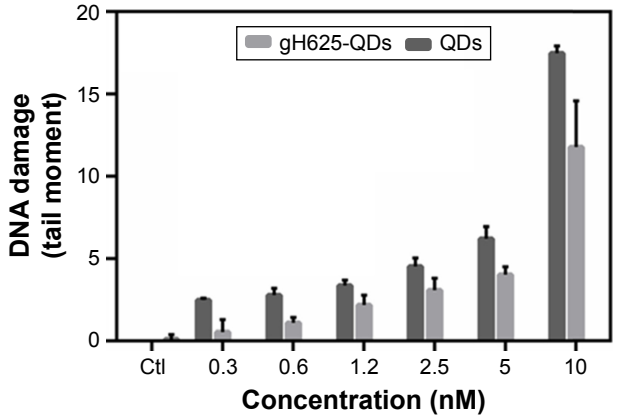


**Figure 3** Comet assay. Histogram of DNA damage of *Daphnia magna* added to QD, with or without gH625. Results are expressed as mean ± SD ($P<0.05$).
**Abbreviations:** QD, quantum dot; SD, standard deviation; Ctl, control.

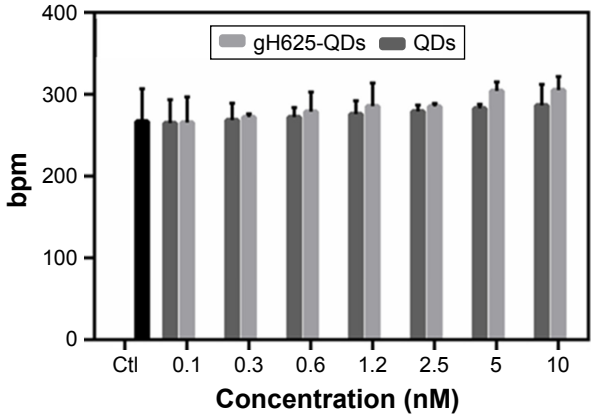


**Figure 4** Observed heart rate of *Daphnia magna* after exposure to QDs and QDs-gH625. The results are relative to average of beats ± SD.
**Abbreviations:** bpm, beats per min; QD, quantum dot; SD, standard deviation; Ctl, control.

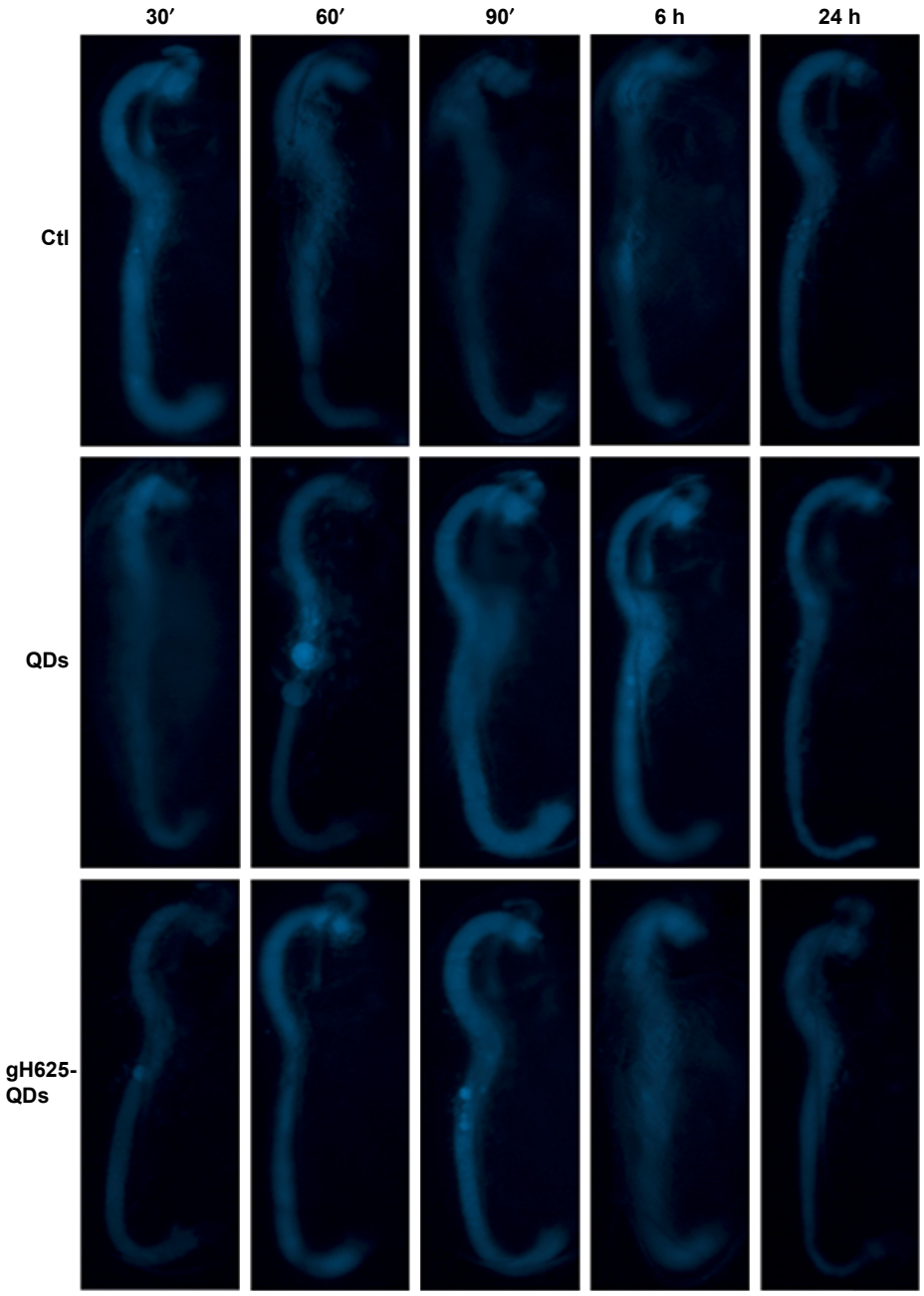


**Figure 5** Fluorescence image of *Daphnia magna* after exposure (30′, 60′, 90′, 6 h and 24 h) to QDs and QDs-gH625 (5 nM).
**Abbreviations:** QD, quantum dot; Ctl, control.

Daphnids were exposed to 5 nM QDs and gH625-QDs for 24 h. After 30′, we noticed no significant differences between the gut of daphnids exposed to QDs or gH625-QDs and controls; at 60′, we started evidencing significant differences with the control. When *D. magna* were exposed to gH625-QDs, we observed that they were not assimilated within the organism, but were concentrated markedly in the gastrointestinal tracts and in brood chamber, whereas the QDs showed a widespread distribution within the body at 60′ and more significantly at 90′. QDs alone were more persistent in the digestive tract and were excreted at 24 h (Figure 5). This persistence could have significant implications in accumulation and toxicity. The uptake of gH625-QDs was clearly different; at 6 h of exposure, we could detect the presence of a small quantity of molecule already. The fluorescence was widespread around the digestive system and within the body, indicating that the QDs are able to enter with a different mechanism.

Equally important as assessing uptake is the need to monitor excretion rates of QDs and gH625-QDs. The inability

to efficiently remove NPs after uptake can lead to accumulation and potential long-term effects. We noticed a consistent excretion of gH625-QDs after 6 h of exposure, with ~15% still remaining in the gut after 24 h. The analysis of samples treated with QDs alone showed a longer persistence of NPs in the gut at 6 h and also at 24 h.

## ROS and antioxidant enzyme analysis

Biochemical biomarkers have been proposed as an early warning indicator of the population-level effect from sublethal concentration exposure. Different responses are reported according to the various test species, the NP characteristics and the exposure condition.

Figure 6 shows the results obtained from experiments on ROS and antioxidant enzymes. In particular, *D. magna* exposed to different doses of QDs and gH625-QDs showed an increase in ROS level relative to controls at 24 h, with no significant difference observed at 48 h (data not shown). Probably, the dose-dependent increase in ROS levels observed in cells after 24 h of exposure to both compounds could be associated with the internalization (Figure 6A). ROS increased on exposure to QDs alone at lower concentrations; instead, gH625-QDs showed a significant increase only from 1.2 nM. In particular, at lower concentrations of gH625-QDs, we observed a lower increase following a dose–response concentration, differently from QDs where the increase began at low concentrations. The antioxidant enzymatic studies were conducted at the same concentration used in the acute bioassay. A concentration-dependent increase in the activity of ROS and CAT was found in experiments on QDs, with SOD also changing with concentration. These results suggest that QD toxicity involves oxidative stress and that SOD activity is a defense mechanism against oxidative stress (Figure 6B and C). The induction of antioxidant enzymes such as CAT and SOD is correlated with observations of oxidative tissue damage and, consequently, also DNA damage. In fact, the induction of CAT usually indicates that $H_2O_2$ excess needs to be decreased to maintain the balance of free radicals in *D. magna*. The reduction of CAT activity determines a balance alteration, and the residual $H_2O_2$ would

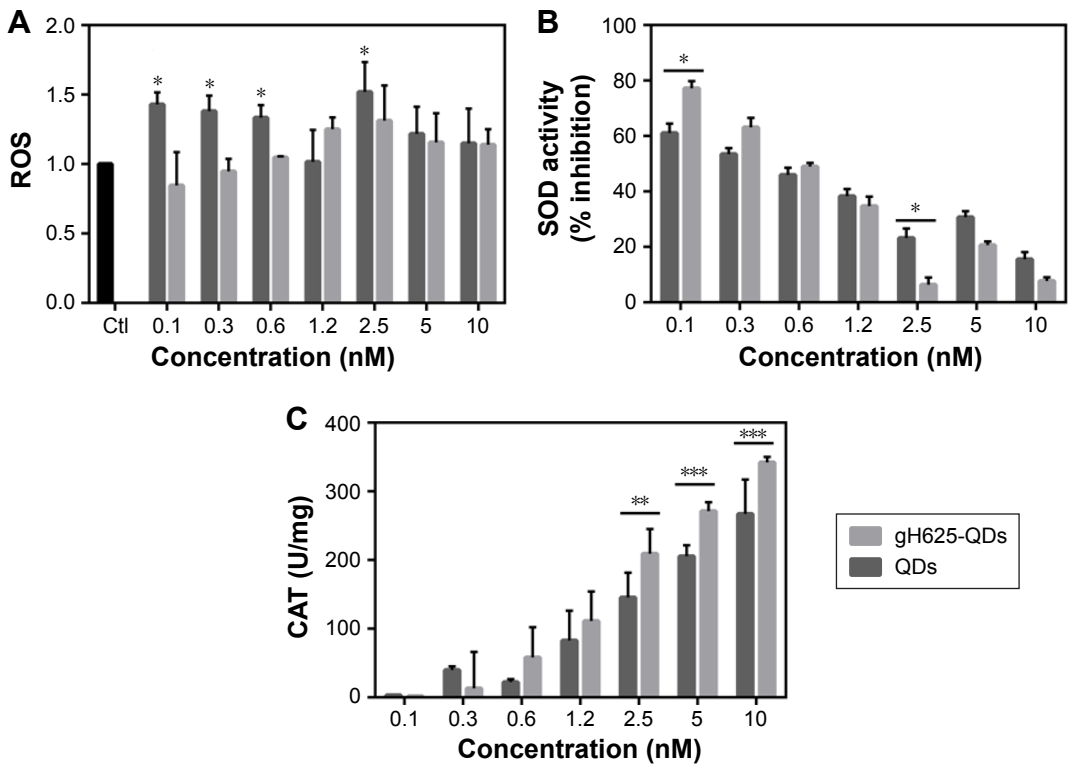


**Figure 6** Response of *Daphnia magna* to oxidative stress on exposure to QDs and gH625-QDs for 24 h.

**Notes:** (**A**) ROS production by dichlorofluorescein fluorescence. Data are given as fluorescence values (mean ± SEM [n=9]). *$P$<0.05, **$P$<0.01 and ***$P$<0.001, Tukey post hoc test following one-way ANOVA versus the control group (Ctl). (**B**) CAT activity is expressed as units* $mg^{-1}$ of protein mean ± SEMs (n=9). *$P$<0.05, **$P$<0.01 and ***$P$<0.001, Bonferroni post hoc test following two-way ANOVA versus the QDs group. (**C**) SOD activity is given as percentage of SOD inhibition compared to the control mean ± SEMs (n=9). *$P$<0.05, **$P$<0.01 and ***$P$<0.001, Bonferroni post hoc test following two-way ANOVA versus the QDs group. All the data show significant differences ($P$<0.05) compared to the control group (Ctl).

**Abbreviations:** ANOVA, analysis of variance; CAT, catalase; QD, quantum dot; ROS, reactive oxygen species; SD, standard deviation; SEM, standard error of the mean; SOD, superoxide dismutase.

**Table 3** Embryotoxic effects in *Xenopus laevis*

| | Ctl | QDs | gH625-QDs |
|---|---|---|---|
| Utilized embryos (n) | 63 | 63 | 63 |
| Dead embryos (n) | 13 | 10 | 13 |
| Living larvae (n) | 50 | 53 | 52 |
| Mortality (%) | 20 | 16 | 18 |

**Note:** The concentration used was 117 nM.
**Abbreviations:** Ctl, control; QDs, quantum dots.

cause damages in *D. magna*. For gH625-QDs, the ROS level remained quite constant, CAT and SOD increased slightly in a dose-dependent manner and there were no significant differences with the controls at 24 and 48 h. In conclusion, there is evidence that ROS promotes CAT and SOD activities in *D. magna*, which is advantageous to prevent too high levels of ROS and subsequent oxidative damage.

## QDs and gH625-QDs effects on *X. laevis*

*X. laevis*, the South African clawed frog, was used to probe the efficacy and potential toxicity of QDs and gH625-QDs on living organisms. Preliminary experiments were performed using 10 nM for both QDs and gH625-QDs. The embryos harvested in the presence of gH625-QDs (n=63), QDs (n=63) and control sibling embryos (n=63) showed a similar percentage of mortality: 18%, 16% and 20%, respectively. The mortality values of treated embryos were not statistically relevant, compared to those of the control sibling embryos (Table 3; Figure 7A). The mortality distributions, evaluated by nonparametric Mantel–Cox test, gave $P>0.05$. In particular, QD treatment compared with the control gave $P=0.484$, while gH625-QD treatment compared with control showed $P=0.612$. Moreover, the relationship between the control and the treated groups was verified by chi-square test and the resulting $P$-value was 0.502 (Table 3). The length (n=90), heartbeat (n=102) and dorsal pigment (n=90) of the treated embryos were not statistically different from the control embryos, showing a $P$-value $>0.05$. As for length, the Mann–Whitney test showed that there was a difference between QD-treated embryos and controls ($P=0.002$). The embryos treated with QDs turned out to be slightly longer than the controls; however, the length was compatible with stage 46 (0.9–1.2 cm; Figure 7B). Heart rate of embryos treated with QDs and gH625-QDs versus control embryos

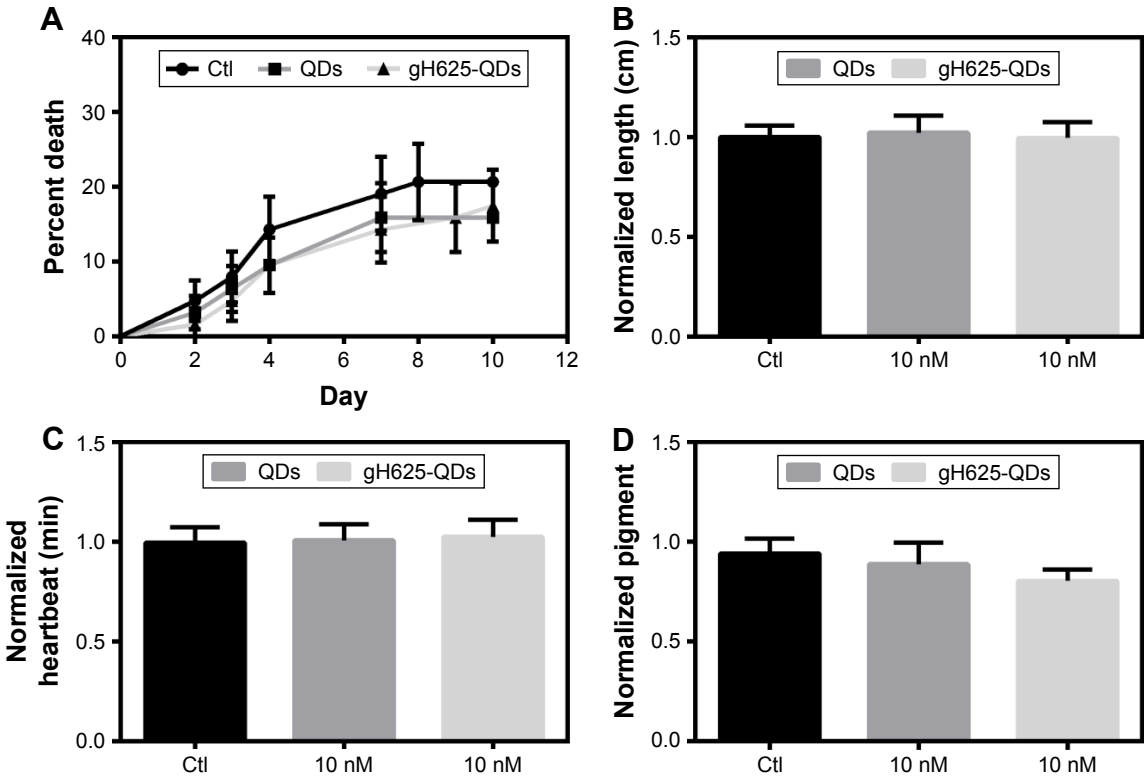


**Figure 7** Embryotoxic parameters in *Xenopus laevis*.
**Notes:** (**A**) Mortality evaluation. The mortality distributions were evaluated by nonparametric Mantel–Cox test, which gave $P>0.05$. (**B**) Growth retardation analysis. The growth retardation was evaluated with ANOVA statistical test, which gave $P>0.05$. (**C**) Observed heart rate of *Xenopus laevis* after exposure to QDs and QDs-gH625. The heartbeat was evaluated with ANOVA statistical test, which gave $P>0.05$. (**D**) Analysis of dorsal pigmentation. The dorsal pigmentation was evaluated with ANOVA statistical test, which gave $P>0.05$. Data are reported as mean ± SD.
**Abbreviations:** ANOVA, analysis of variance; QDs, quantum dots; SD, standard deviation; Ctl, control.

showed $P>0.05$ (Figure 7C). The same results were obtained in dorsal pigmentation (Figure 7D).

In detail, the controls, QD and gH625-QD groups had average lengths of 0.98, 1.02 and 0.96 cm, respectively. The average of heart rate was 110 $min^{-1}$ for all groups. The average quantity of dorsal pigment of embryos was ~15% for controls and QDs, while it was 13% for gH625-QDs. The toxicity parameters used in this study (body length, hearth rate and quantity of dorsal pigmentation) were similar in gH625-QDs, QDs and control embryos. These results show that QDs have no toxic effects on *X. laevis* embryogenesis at the concentrations used in these experiments.

## gH625-QDs and QDs localization in *X. laevis*

The images obtained from confocal microscopy (Figure 8) of the sectioned embryos showed that both QDs and gH625-QDs were visible in the primordium of lung (Figure 8B and C), in the gills (Figure 8H and I) and in the intestine (Figure 8D–F). gH625-QDs in the primordium of lung appeared as spots of different sizes that thickened in small defined highly fluorescent areas (Figure 8C, arrows) in contrast to naked QDs (Figure 8B, asterisks) that were visible in the form of widespread dots (aggregates). They were distributed on the alveolar septa (Figure 8B and C). Similar localization of QDs and gH625-QDs were detectable on the branches of the gills (Figure 8H and I, arrows). gH625-QDs were also detected as spots in different tracts of the intestine, in particular, in the stomach (Figure 8D, st), duodenum (Figure 8D and F; du) and some tract of the small intestine (Figure 8D and E; il). *Xenopus* brain autofluorescence at 543 nm made it difficult to specifically describe the localization in the brain; nonetheless, fluorescent gH625-QDs were detectable in some areas as small spots (Figure 8G, asterisks). We did not evidence any localization in the heart (Figure 8J–L).

# Discussion

Nanomaterials are used in a variety of medical applications, offering a unique chance to overcome biologic barriers and release bioactive moieties to specific intracellular targets. However, their use is hampered by their potential toxicity, and the use of specific bioassays for assessment of toxicity before starting in vivo studies on mammals represents an important issue. Enhanced and targeted uptakes are the other two key points to consider when designing new drugs and to address before starting in vivo experiments on mammals. The combined use of *D. magna*, *X. laevis* and mammalian models may allow a fuller understanding of several diseases.

*D. magna* is a well-known and ecologically important invertebrate species that has been extensively used as a toxicity test organism for many international standards and guidelines on toxicity tests. The most likely pathway of absorption in *D. magna* is through active filter feeding. Both ingestion and excretion in *D. magna* are very fast;[30] it has been reported that the gut repeatedly filled with NPs associated with food source with 30 min of exposure is able to excrete them within 48 h.[61] In our experiments, we observed accumulated QDs in the digestive tract, which is the main uptake route in aquatic invertebrates, and confirmed that ingestion is the major mechanism of uptake. After 24 h, their presence is significantly reduced, indicating they are excreted. Corresponding images collected for gH625-QDs showed a widespread distribution around the digestive system and within the body, probably indicating that functionalized QDs also reach other compartments of the organism and are much more excreted; the opposite was observed for QDs alone. In fact, images collected for QDs showed that even after 24 h, a significantly higher number of NPs was retained. The persistence of NPs within the digestive tract may have significant implications with respect to toxicity and, indeed, lower excretion processes may be correlated with higher toxicity. The comet assay showed a dose-dependent increase in DNA migration in *D. magna* exposed to QDs and gH625-QDs. QDs functionalized with gH625 were able to induce lower DNA damage than QDs alone at each concentration considered. We showed that DNA damage in *D. magna* induced by NPs could be evaluated by the comet assay with great sensitivity, making it a useful tool for genotoxicity test of chemicals and for assessment of genotoxicity potential.

Thus, to evaluate the toxicity of QDs functionalized with gH625, we also measured in vivo ROS generation and DNA damage. Oxidative stress is a widely used cellular molecular response to exposure of NPs and may not only indicate damage and cellular repair but also a physical response to a foreign object. Recently, Kim et al[62] showed that the toxicity of MNPs was mediated by ROS generation through oxidative stress. The increased toxicity was attributed to accumulation of MNPs in the intestine of *Daphnia*. Generation of ROS by naked QDs has also been reported by Lovric et al[63] and, indeed, we observed an increased ROS generation in a dose-dependent manner upon exposure to QDs. On the contrary, we showed that QDs functionalized with gH625 were able to induce ROS generation to a lower extent. In addition, the production of ROS and the enzymatic responses of CAT and SOD in *D. magna* showed a concentration-dependent

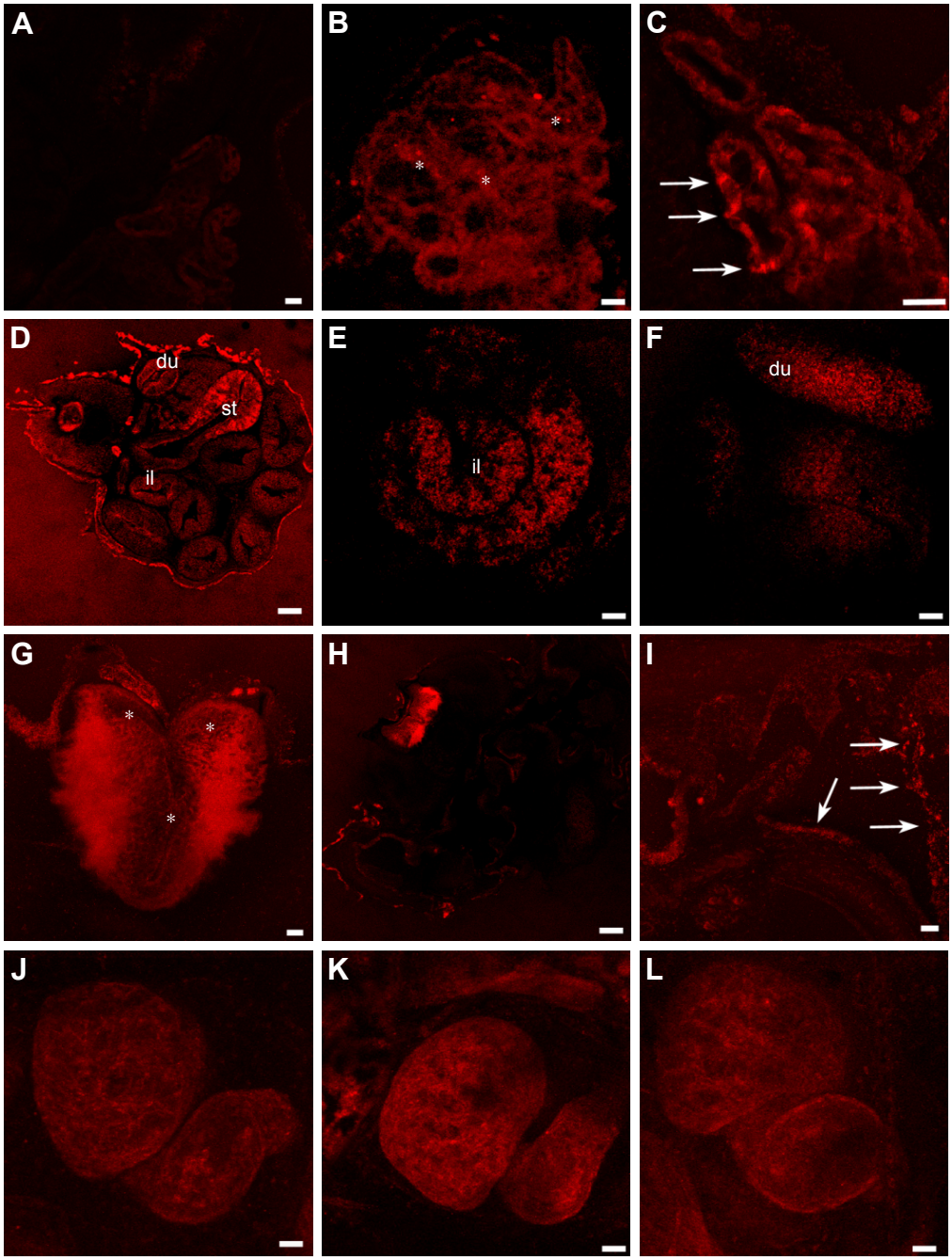


**Figure 8** gH625-QDs confocal localization in stage 46 *Xenopus laevis* embryos.
**Notes:** (**A**) Control section. (**B, C**) Optical sections of primordium of lung treated with (**B**) naked QDs and (**C**) gH625-QDs. QDs localize in the form of widespread dots (**B**, asterisks) in contrast gH625-QDs, which are disposed in small fluorescent areas (**C**, arrows). In the intestine (**D**–**F**), gH625-QDs are visible only in some stretches: st, du and il. Hindbrain shows a slight localization of gH625-QDs (**G**, asterisks). (**H**) QDs are barely visible in the gills (**I**) gH625-QDs have a distribution similar to the gills (arrows). (**J**–**L**) QDs and gH626-QDs are not visible in the heart. Bars: (**A**–**C**, **G**, **I**) =20 μm; (**E, F, K, J, L**) =50 μm; (**H**) =100 μm; (**D**) =200 μm.
**Abbreviations:** du, duodenum; il, ileum; QDs, quantum dots; st, stomach.

increase; ROS production in gH625-QDs was less significant and CAT induction increased as a response to ROS generated. These results indicate that both QDs and gH625-QDs could generate ROS through various biochemical processes, which also lead to the development of a series of defense mechanisms, such as CAT and SOD; by the way, the passage of time could also lead to genotoxic damage due to accumulation of ROS.

Furthermore, the induction of DNA lesions was correlated to an increase of ROS and CAT and SOD, suggesting that production of ROS was involved in the genotoxicity of QDs. For gH625-QDs, we noticed a lower genotoxicity and lower

ROS production, even if there was an activation of SOD and CAT. Altogether these observations, including accumulation and excretion, indicate a more widespread uptake of functionalized QDs compared to naked QDs coupled with a lower toxicity, a lower generation of oxidative stress and a lower genotoxicity.

Amphibian embryos have been used as an alternative vertebrate animal model for the discovery of potential therapeutic agents; moreover, a close similarity to mammals is present at the level of organ organization and structure. As a matter of fact, a significant conservation in nephron organization between the kidneys of *Xenopus* embryos and adult mice was demonstrated in a large-scale comparative gene expression study.[64] Our data clearly show that both QDs and gH625-QDs do not affect the survival of embryos. The embryonic phenotype, observed in the stereomicroscope, appears unaltered for both gH625-QDs and QDs. Small modifications are compatible with wild-type phenotype. Embryos of stage 46 harvested in the presence of gH625-QDs and QDs, showing that they are mainly localized in the gills, in the primordium lung and in the intestine. Although the localization is similar, a deeper analysis shows great differences both in the lung and gills. QDs generally show a widespread localization in the form of spots everywhere. In contrast, for gH625-QDs, we evidenced their presence in the form of spots of different sizes that thickened in small defined areas on the alveolar septa of lung and on branches of the gills. In these organs, the internalized gH625-QDs were four times higher than the QDs. Amphibians use many different organs for gas exchange throughout their lives, including internal/external gills, lungs and skin. Gills, the primary respiration organ of tadpoles, whose function is extraction of oxygen from water and excretion of carbon dioxide, usually consist of thin filaments of tissue, branches or slender tufted processes, which have a highly folded surface to increase the surface area. A high surface area is crucial for an effective gas exchange.[65] *Xenopus* lung is constituted by peribronchial vessels that form connections between the pulmonary artery and vein at the base of the lung. Shortly after hatching, *X. laevis* tadpoles fill their lungs with air. The early lung use is important in determining the probability of a successful metamorphosis.[66,67] Before metamorphosis, *Xenopus* lung development at the cellular and molecular levels is comparable to embryonic stages of mouse respiratory system development between embryonic days 8.5 and 10.5. Therefore, it could be considered as a model to define the programs controlling early respiratory system development.[68]

At stage 40/41, *X. laevis* embryos opened their mouth and ingestion became the main route of QDs intake. Thus, the number of ingested particles increased because in the following days, the grazing behavior of the larvae became very active. The treated embryos showed a high concentration of gH625-QDs as spots in some stretches of the intestine, such as stomach, duodenum and partially ileum. In general, the intestinal mucosa is delegated to the absorption, in particular, at the level of the small intestine where the brush border is present. These sites may facilitate the absorption of gH625-QDs. The entire digestive tract from the esophagus to the colon, as well as the epithelial component of the digestive and respiratory organs, including the lung, is derived from the endoderm both in mammals and *Xenopus*. *Xenopus* is a good model to understand the murine endoderm production because the morphologic and molecular mechanisms used to produce this embryonic germ layer are similar; thus, it is possible to transfer the data obtained in *Xenopus* to mammals.[69]

Finally, we strongly support the view that gH625-QDs localize in the rhombencephalon, even though the autofluorescence makes it difficult to describe the localization in detail. gH625-QDs and QDs are not visible in the heart. These preliminary studies show that both QDs and gH625-QDs are not toxic for *Xenopus* embryos. Our data showed that they are adsorbed by some organs such as primordium of lung, gills and intestine, but the functionalized QDs showed a different concentration and distribution compared to naked QDs, confirming that gH625 facilitates the adhesion of QDs to the wall of these organs and possibly their internalization.

Our studies further demonstrate that these data could be transferred to the mammalian model and represent an alternative for preliminary screening of novel drugs, reducing the high costs as well as the logistic and ethical problems involved in the use of mice, rats and rabbits as model organisms for in vivo studies.

## Acknowledgment

We thank Luca De Luca (Institute of Biostructure and Bioimaging, Italian National Research Council, Naples, Italy) for technical assistance.

## Disclosure

The authors report no conflicts of interest in this work.

## References

1. Grever MR. Accelerating safe drug development: an ideal approach to approval. *Hematology Am Soc Hematol Educ Program*. 2013;2013:24–29.

2. Pietro PD, Strano G, Zuccarello L, Satriano C. Gold and silver nanoparticles for applications in theranostics. *Curr Top Med Chem*. 2016; 16(27):3069–3102.
3. Anchordoquy TJ, Barenholz Y, Boraschi D, et al. Mechanisms and barriers in cancer nanomedicine: addressing challenges, looking for solutions. *ACS Nano*. 2017;11(1):12–18.
4. Sahandi Zangabad P, Karimi M, Mehdizadeh F, et al. Nanocaged platforms: modification, drug delivery and nanotoxicity. Opening synthetic cages to release the tiger. *Nanoscale*. 2017;9(4):1356–1392.
5. Biffi S, Andolfi L, Caltagirone C, et al. Cubosomes for in vivo fluorescence lifetime imaging. *Nanotechnology*. 2017;28(5):055102.
6. Becker D, Brinkmann BF, Zeis B, Paul RJ. Acute changes in temperature or oxygen availability induce ROS fluctuations in *Daphnia magna* linked with fluctuations of reduced and oxidized glutathione, catalase activity and gene (haemoglobin) expression. *Biol Cell*. 2011;103(8):351–363.
7. Carberry TP, Tarallo R, Falanga A, et al. Dendrimer functionalization with a membrane-interacting domain of herpes simplex virus type 1: towards intracellular delivery. *Chemistry*. 2012;18(43):13678–13685.
8. Galdiero S, Falanga A, Vitiello M, et al. Exploitation of viral properties for intracellular delivery. *J Pept Sci*. 2014;20(7):468–478.
9. Galdiero S, Falanga A, Morelli G, Galdiero M. gH625: a milestone in understanding the many roles of membranotropic peptides. *Biochim Biophys Acta*. 2015;1848(1 Pt A):16–25.
10. Galdiero S, Falanga A, Vitiello M, et al. The presence of a single N-terminal histidine residue enhances the fusogenic properties of a membranotropic peptide derived from herpes simplex virus type 1 glycoprotein H. *J Biol Chem*. 2010;285(22):17123–17136.
11. Galdiero S, Falanga A, Vitiello M, et al. Peptides containing membrane-interacting motifs inhibit herpes simplex virus type 1 infectivity. *Peptides*. 2008;29(9):1461–1471.
12. Tarallo R, Accardo A, Falanga A, et al. Clickable functionalization of liposomes with the gH625 peptide from Herpes simplex virus type I for intracellular drug delivery. *Chemistry*. 2011;17(45):12659–12668.
13. Borchmann DE, Tarallo R, Avendano S, et al. Membranotropic peptide-functionalized poly(lactide)-graft-poly(ethylene glycol) brush copolymers for intracellular delivery. *Macromolecules*. 2015;48(4): 942–949.
14. Falanga A, Tarallo R, Carberry T, Galdiero M, Weck M, Galdiero S. Elucidation of the interaction mechanism with liposomes of gH625-peptide functionalized dendrimers. *PLoS One*. 2014;9(11):e112128.
15. Tarallo R, Carberry TP, Falanga A, et al. Dendrimers functionalized with membrane-interacting peptides for viral inhibition. *Int J Nanomedicine*. 2013;8:521–534.
16. Perillo E, Allard-Vannier E, Falanga A, et al. Quantitative and qualitative effect of gH625 on the nanoliposome-mediated delivery of mitoxantrone anticancer drug to HeLa cells. *Int J Pharm*. 2015;488(1–2):59–66.
17. Perillo E, Porto S, Falanga A, et al. Liposome armed with herpes virus-derived gH625 peptide to overcome doxorubicin resistance in lung adenocarcinoma cell lines. *Oncotarget*. 2016;7(4):4077–4092.
18. Valiante S, Falanga A, Cigliano L, et al. Peptide gH625 enters into neuron and astrocyte cell lines and crosses the blood-brain barrier in rats. *Int J Nanomedicine*. 2015;10:1885–1898.
19. Smyder JA, Krauss TD. Coming attractions for semiconductor quantum dots. *Mater Today*. 2011;14(9):382–387.
20. Falanga A, Vitiello MT, Cantisani M, et al. A peptide derived from herpes simplex virus type 1 glycoprotein H: membrane translocation and applications to the delivery of quantum dots. *Nanomedicine*. 2011; 7(6):925–934.
21. Aruoja V, Dubourguier HC, Kasemets K, Kahru A. Toxicity of nanoparticles of CuO, ZnO and $TiO_2$ to microalgae Pseudokirchneriella subcapitata. *Sci Total Environ*. 2009;407(4):1461–1468.
22. Kasemets K, Ivask A, Dubourguier HC, Kahru A. Toxicity of nanoparticles of ZnO, CuO and $TiO_2$ to yeast Saccharomyces cerevisiae. *Toxicol In Vitro*. 2009;23(6):1116–1122.
23. Ivask A, Kurvet I, Kasemets K, et al. Size-dependent toxicity of silver nanoparticles to bacteria, yeast, algae, crustaceans and mammalian cells in vitro. *PLoS One*. 2014;9(7):e102108.
24. Ozel RE, Alkasir RS, Ray K, Wallace KN, Andreescu S. Comparative evaluation of intestinal nitric oxide in embryonic zebrafish exposed to metal oxide nanoparticles. *Small*. 2013;9(24):4250–4261.
25. Bacchetta R, Santo N, Fascio U, et al. Nano-sized CuO, $TiO_2$ and ZnO affect *Xenopus laevis* development. *Nanotoxicology*. 2012;6(4): 381–398.
26. Vecchio G, Galeone A, Brunetti V, et al. Concentration-dependent, size-independent toxicity of citrate capped AuNPs in *Drosophila melanogaster*. *PLoS One*. 2012;7(1):e29980.
27. Pompa PP, Vecchio G, Galeone A, et al. Physical assessment of toxicology at nanoscale: nano dose-metrics and toxicity factor. *Nanoscale*. 2011;3(7):2889–2897.
28. Zhang XD, Wu HY, Wu D, et al. Toxicologic effects of gold nanoparticles in vivo by different administration routes. *Int J Nanomedicine*. 2010;5:771–781.
29. Yeoman MS, Faragher RG. Ageing and the nervous system: insights from studies on invertebrates. *Biogerontology*. 2001;2(2):85–97.
30. Baun A, Hartmann NB, Grieger K, Kusk KO. Ecotoxicity of engineered nanoparticles to aquatic invertebrates: a brief review and recommendations for future toxicity testing. *Ecotoxicology*. 2008;17(5): 387–395.
31. Lovern SB, Owen HA, Klaper R. Electron microscopy of gold nanoparticle intake in the gut of *Daphnia magna*. *Nanotoxicology*. 2008; 2(1):43–48.
32. Corotto F, Ceballos D, Lee A, Vinson L. Making the most of the *Daphnia* heart rate lab: optimizing the use of ethanol, nicotine & caffeine. *Am Biol Teach*. 2010;72(3):176–179.
33. Chapman MA, Lewis MH. *An Introduction to the Freshwater Crustacea of New Zealand*. *Dr Richard Hamond's Library*. Auckland: Collins; 1976;1–261.
34. Paul RJ, Colmorgen M, Hüller S, Tyroller F, Zinkler D. Circulation and respiratory control in millimetre-sized animals (*Daphnia magna*, Folsomia candida) studied by optical methods. *J Comp Physiol B*. 1997;167(6):399–408.
35. Colmorgen M, Paul RJ. Imaging of physiological functions in transparent animals (Agonus cataphractus, *Daphnia magna*, Pholcus phalangioides) by video microscopy and digital image processing. *Comp Biochem Physiol A: Physiol*. 1995;111(4):583–595.
36. Tamplin OJ, White RM, Jing L, et al. Small molecule screening in zebrafish: swimming in potential drug therapies. *Wiley Interdiscip Rev Dev Biol*. 2012;1(3):459–468.
37. Takagi C, Sakamaki K, Morita H, et al. Transgenic *Xenopus laevis* for live imaging in cell and developmental biology. *Dev Growth Differ*. 2013;55(4):422–433.
38. Tomlinson ML, Field RA, Wheeler GN. *Xenopus* as a model organism in developmental chemical genetic screens. *Mol Biosyst*. 2005;1(3): 223–228.
39. Brändli AW. Prospects for the *Xenopus* embryo model in therapeutics technologies. *CHIMIA Int J Chem*. 2004;58(10):694–702.
40. Wheeler GN, Brandli AW. Simple vertebrate models for chemical genetics and drug discovery screens: lessons from zebrafish and *Xenopus*. *Dev Dyn*. 2009;238(6):1287–1308.
41. Elendt BP, Bias WR. Trace nutrient deficiency in *Daphnia magna* cultured in standard medium for toxicity testing. Effects of the optimization of culture conditions on life history parameters of *D. magna*. *Water Res*. 1990;24(9):1157–1167.
42. ISO10870. Water quality – guidelines for the selection of sampling methods and devices for benthic macroinvertebrates in fresh waters. BSI; Geneva: International Organization for Standardization; 2012.
43. ISO6341. Water quality – determination of the inhibition of the mobility of *Daphnia magna* Straus (Cladocera, Crustacea) – acute toxicity test; Geneva: International Organization for Standardization; 2012.
44. Kim J, Park Y, Yoon TH, Yoon CS, Choi K. Phototoxicity of CdSe/ZnSe quantum dots with surface coatings of 3-mercaptopropionic acid or tri-n-octylphosphine oxide/gum arabic in *Daphnia magna* under environmentally relevant UV-B light. *Aquat Toxicol*. 2010;97(2): 116–124.

45. Kim MJ, Park C, Choi K, Yoon TH. Implications of "Trap Emission" observed from quantum dot nanoparticles accumulated in toxicity test organism, *Daphnia magna*. *Bull Korean Chem Soc*. 2008;29(6):1101–1102.
46. Xie F, Koziar SA, Lampi MA, et al. Assessment of the toxicity of mixtures of copper, 9,10-phenanthrenequinone, and phenanthrene to *Daphnia magna*: evidence for a reactive oxygen mechanism. *Environ Toxicol Chem*. 2006;25(2):613–622.
47. Bradford MM. A rapid and sensitive method for the quantitation of microgram quantities of protein utilizing the principle of protein-dye binding. *Anal Biochem*. 1976;72:248–254.
48. Galdiero E, Maselli V, Falanga A, et al. Integrated analysis of the ecotoxicological and genotoxic effects of the antimicrobial peptide melittin on *Daphnia magna* and Pseudokirchneriella subcapitata. *Environ Pollut*. 2015;203:145–152.
49. Baylor ER. Cardiac pharmacology of the cladoceran, Daphnia. *Biol Bull*. 1942;83(2):165–172.
50. Nieuwkoop P, Faber J. Normal table of *Xenopus laevis* (Daudin): a systematical and chronological survey of the development from the fertilized egg till the end of metamorphosis/edited by PD Nieuwkoop and J Faber. *Hubrecht-Laboratorium (Embryologisch Instituut)* Amsterdam: North-Holland Pub. Co., 1967;1–260.
51. Shapiro SS, Wilk MB. An analysis of variance test for normality (complete samples). *Biometrika*. 1965;52(3/4):591–611.
52. Kolmogoroff A. Confidence limits for an unknown distribution function. *Ann Math Statist*. 1941;12(4):461–463.
53. Kruskal WH, Wallis WA. Use of ranks in one-criterion variance analysis. *J Am Stat Assoc*. 1952;47(260):583–621.
54. Tussellino M, Ronca R, Formiggini F, et al. Polystyrene nanoparticles affect *Xenopus laevis* development. *J Nanopart Res*. 2015;17(2):1–17.
55. Lovell DP, Omori T. Statistical issues in the use of the comet assay. *Mutagenesis*. 2008;23(3):171–182.
56. Paul RJ, Colmorgen M, Pirow R, Chen YH, Tsai MC. Systemic and metabolic responses in *Daphnia magna* to anoxia. *Comp Biochem Physiol A: Mol Integr Physiol*. 1998;120(3):519–530.
57. Lamkemeyer T, Zeis B, Paul RJ. Temperature acclimation influences temperature-related behaviour as well as oxygen-transport physiology and biochemistry in the water flea *Daphnia magna*. *Can J Zool*. 2003; 81(2):237–249.
58. Campbell AK, Wann KT, Matthews SB. Lactose causes heart arrhythmia in the water flea Daphnia pulex. *Comp Biochem Physiol B Biochem Mol Biol*. 2004;139(2):225–234.
59. Jeong TY, Kim HY, Kim SD. Multi-generational effects of propranolol on *Daphnia magna* at different environmental concentrations. *Environ Pollut*. 2015;206:188–194.
60. Feswick A, Griffitt RJ, Siebein K, Barber DS. Uptake, retention and internalization of quantum dots in Daphnia is influenced by particle surface functionalization. *Aquat Toxicol*. 2013;130–131:210–218.
61. Lovern SB, Klaper R. *Daphnia magna* mortality when exposed to titanium dioxide and fullerene (C60) nanoparticles. *Environ Toxicol Chem*. 2006;25(4):1132–1137.
62. Kim KT, Klaine SJ, Cho J, Kim SH, Kim SD. Oxidative stress responses of *Daphnia magna* exposed to TiO(2) nanoparticles according to size fraction. *Sci Total Environ*. 2010;408(10):2268–2272.
63. Lovric J, Cho SJ, Winnik FM, Maysinger D. Unmodified cadmium telluride quantum dots induce reactive oxygen species formation leading to multiple organelle damage and cell death. *Chem Biol*. 2005; 12(11):1227–1234.
64. Raciti D, Reggiani L, Geffers L, et al. Organization of the pronephric kidney revealed by large-scale gene expression mapping. *Genome Biol*. 2008;9(5):R84.
65. Saltys HA, Jonz MG, Nurse CA. Comparative study of gill neuroepithelial cells and their innervation in teleosts and *Xenopus* tadpoles. *Cell Tissue Res*. 2006;323(1):1–10.
66. Smith DG, Rapson L. Differences in pulmonary microvascular anatomy between Bufo marinus and *Xenopus laevis*. *Cell Tissue Res*. 1977;178(1):1–15.
67. Rose CS, James B. Plasticity of lung development in the amphibian, *Xenopus laevis*. *Biol Open*. 2013;2(12):1324–1335.
68. Rankin SA, Thi Tran H, Wlizla M, et al. A Molecular atlas of *Xenopus* respiratory system development. *Dev Dyn*. 2015;244(1):69–85.
69. Tremblay KD. Formation of the murine endoderm: lessons from the mouse, frog, fish, and chick. *Prog Mol Biol Transl Sci*. 2010; 96:1–34.